Electronic Supplementary Information

for

Film formation from plasma-enabled surface-catalyzed dehalogenative coupling of a small organic molecule

Hugo Hartl,[a] Yanru Guo,[a,b] Ken Ostrikov,[a,c] Yubin Xian,[d] Jie Zheng,[b] Xingguo Li,[b] Kathryn E. Fairfull-Smith,[a] Jennifer MacLeod [a*]

a. School of Chemistry, Physics and Mechanical Engineering, Queensland University of Technology (QUT), 2 George Street, Brisbane, QLD, Australia 4000. b. Beijing National
b. Laboratory for Molecular Sciences (BNLMS) College of Chemistry and Molecular Engineering Peking University Beijing 100871, P. R. China c. CSIRO-
c. QUT Joint Sustainable Processes and Devices Laboratory, P. O. Box 218, Lindfield, NSW, 2070, Australia
d. State Key Laboratory of Advanced Electromagnetic Engineering and Technology, School of Electrical and Electronic Engineering, Huazhong University of Science and Technology, Wuhan, Hubei, 430074, People's Republic of China

Contents

Additional characterisation of Si substrate samples

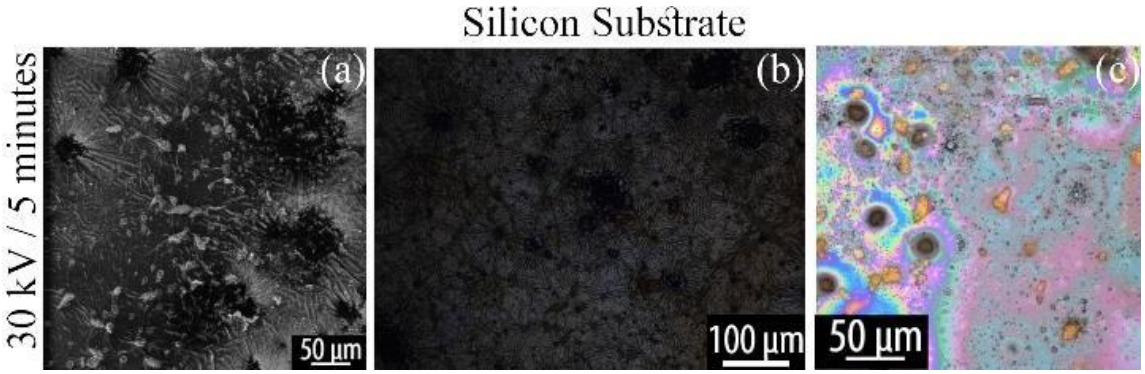

Fig. A.1 (a) HIM image (b) optical image and (c) optical profilometer image of plasma reacted TCB on Si substrate.

Photograph of plasma setup

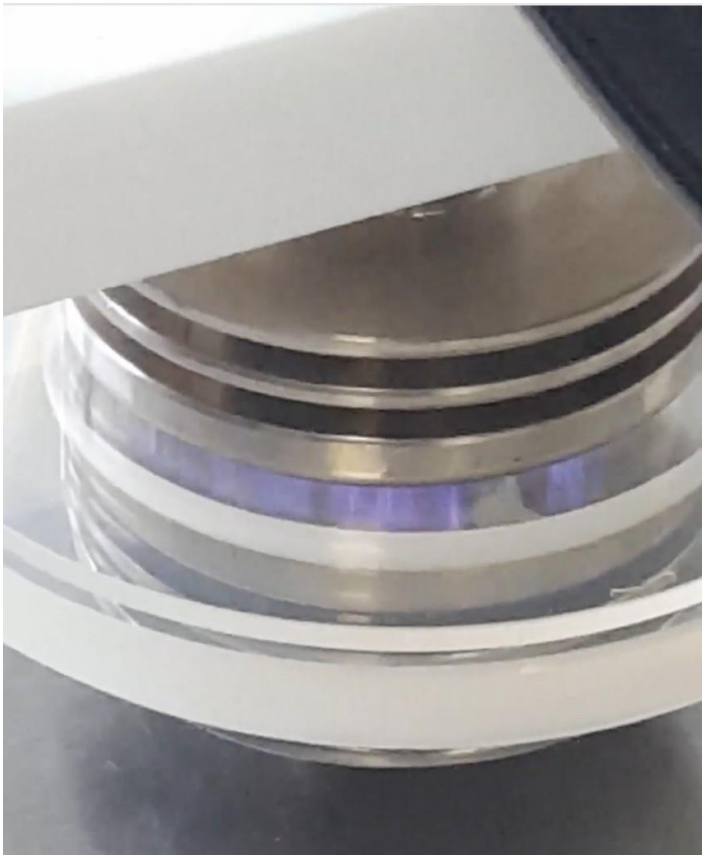

Fig. A.2 Photograph of the plasma setup used in this paper.

Typical oscilloscope trace for the 30 kV plasma

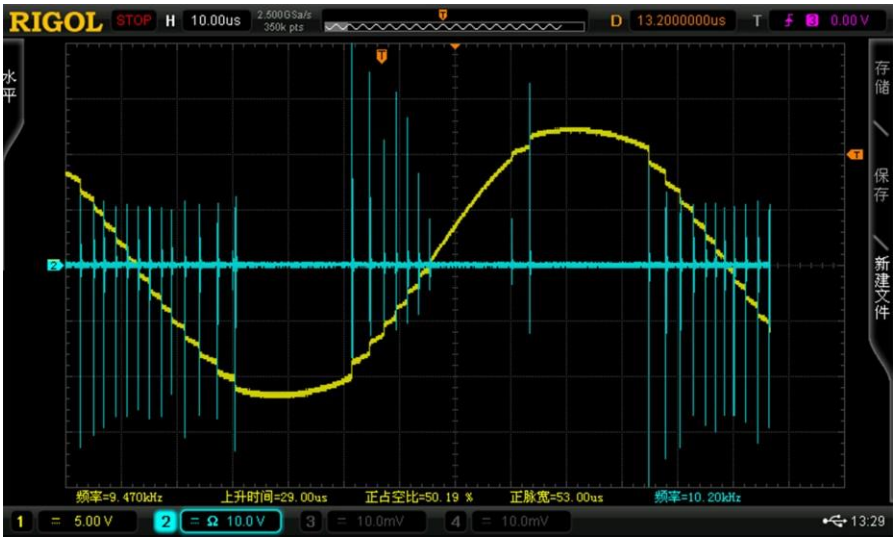

Fig. A.3 Screen capture of the typical waveform of a 30 kV plasma produced in this experimental setup.

Optical profilometer images of the constant-time samples

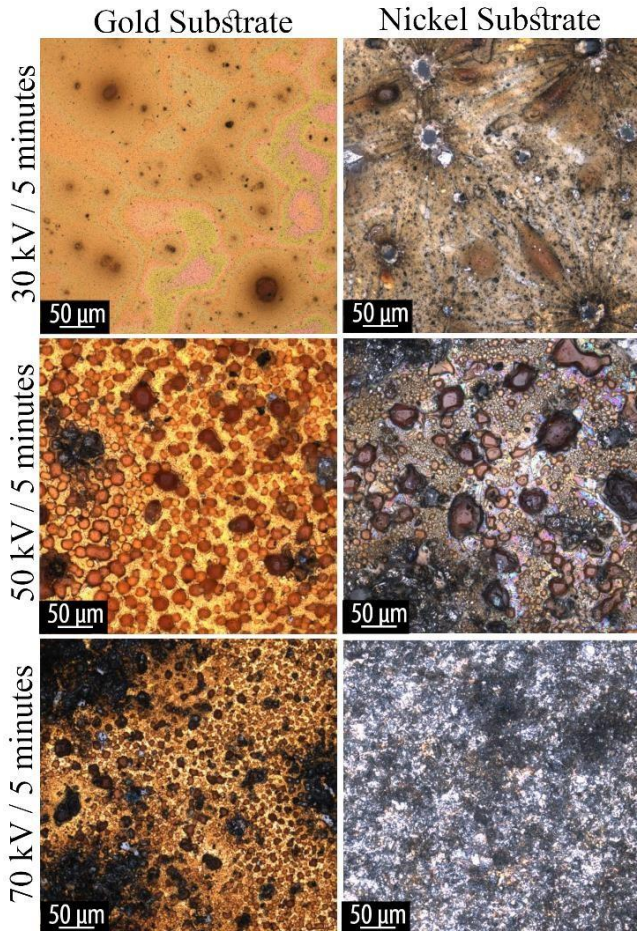

Fig. A.4 Optical profilometer images of constant time samples.

Optical profilometer images of the constant-dose samples

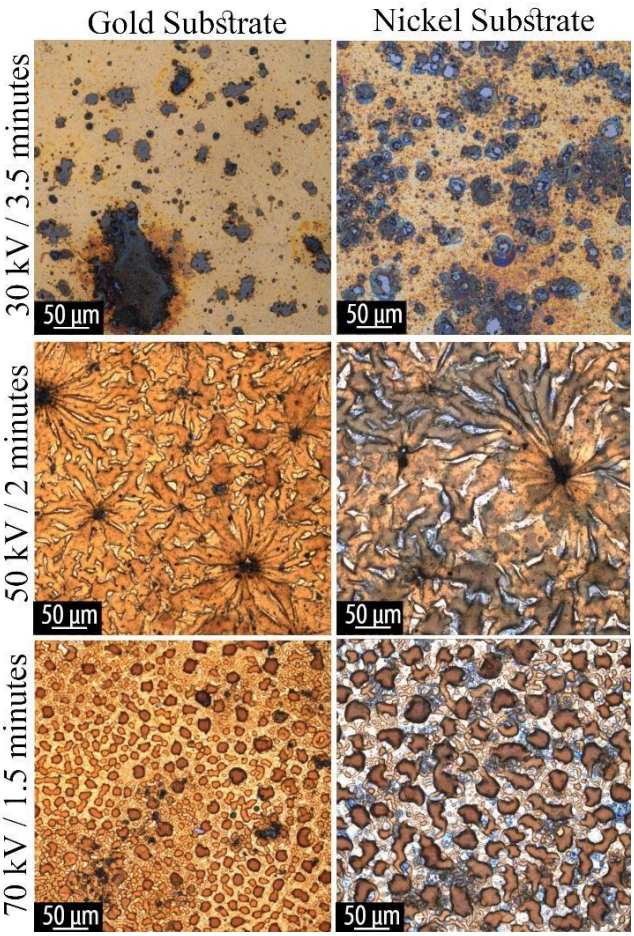

Fig. A.5 Optical profilometer images of constant dose samples.

Photographs of precursor droplets on nickel and gold samples

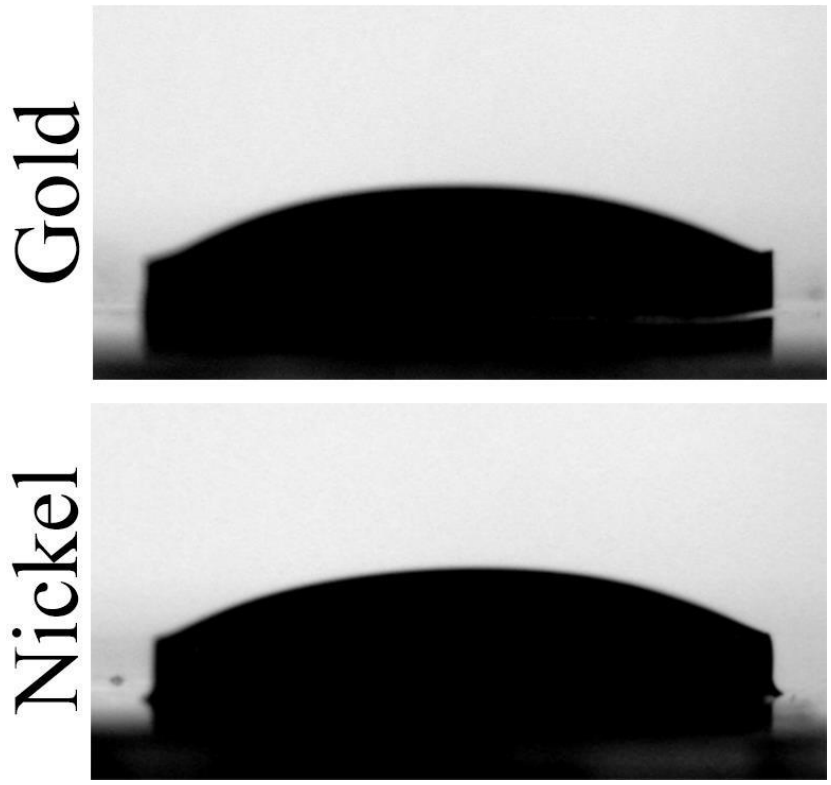

Fig. A.6 TCB liquid droplet on Au and Ni substrate during deposition step, showing that the droplet wets the surface of both metal films. For both films, the maximum thickness was measured via ImageJ at ~0.5 mm. ImageJ was calibrated using the known substrate width of 5 mm.

Additional XPS data

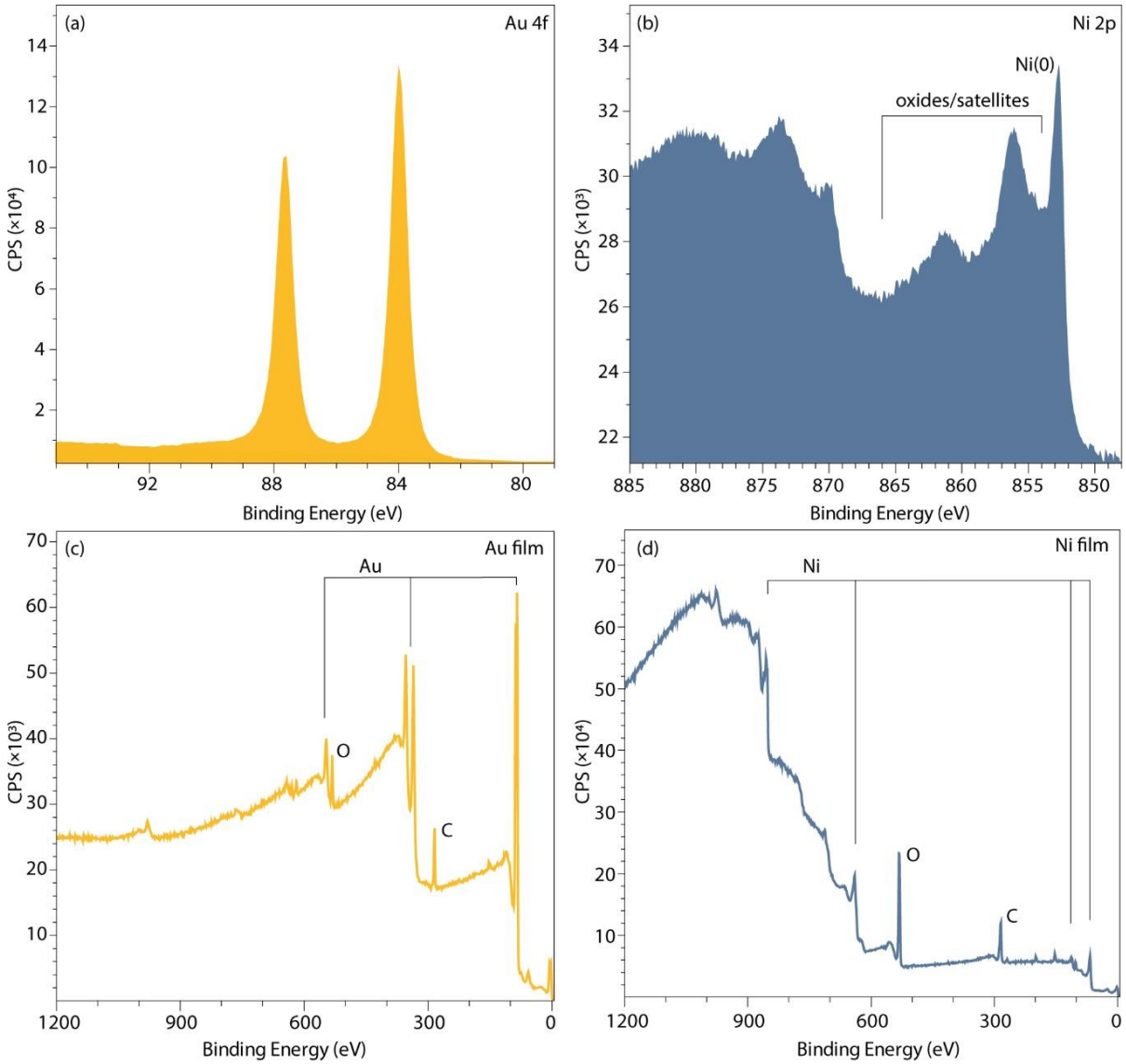

Fig. A.7 XPS scans of as-prepared metal films showing (a) the Au 4f region and (b) the Ni 2p region, (c) survey spectrum of the gold film and (d) survey spectrum of the nickel film.

The Au 4f peaks shown in (a) are well-defined and sharp, and each of the spin-orbit components can be fit with a single asymmetric synthetic peak. This indicates that the gold is metallic, and that no oxide is present. In addition to the expected metal peaks, the survey spectrum (c) shows the presence of both carbon and oxygen, which we attribute to adventitious carbon.

In contrast, the Ni 2p region shown in (b) contains a number of contributions. Ni 2p is notoriously difficult to fit, so synthetic fits are not included here. The sharp metallic peak of Ni 2p3/2 is evident at 852.8 eV; in a clean, oxide-free Ni sample this would be accompanied by two well-defined satellite features at binding energies ~3.7 and ~6 eV higher than the primary peak.[1] Here, there are clearly other contributions present, indicating that Ni exists in additional oxidation states. These states likely arise from NiO and $Ni(OH)_2$, which are typically observed in air-exposed Ni (e.g., as-received Ni powders).[2] The survey spectrum in

(d) shows a strong oxygen contribution, which corroborates the presence of these oxygen-containing nickel phases. As in the gold survey spectrum, some of the observed oxygen is likely associated with adventitious carbon, however we note the relative abundance of oxygen with respect to carbon, and attribute surplus oxygen to nickel oxides.

We note that the survey spectrum of Ni contains a small (ca. 1-2%) contribution from chlorine. This may be due to cross-contamination from polymer film samples during storage.

Determination of rotational and vibrational temperatures in the plasmas

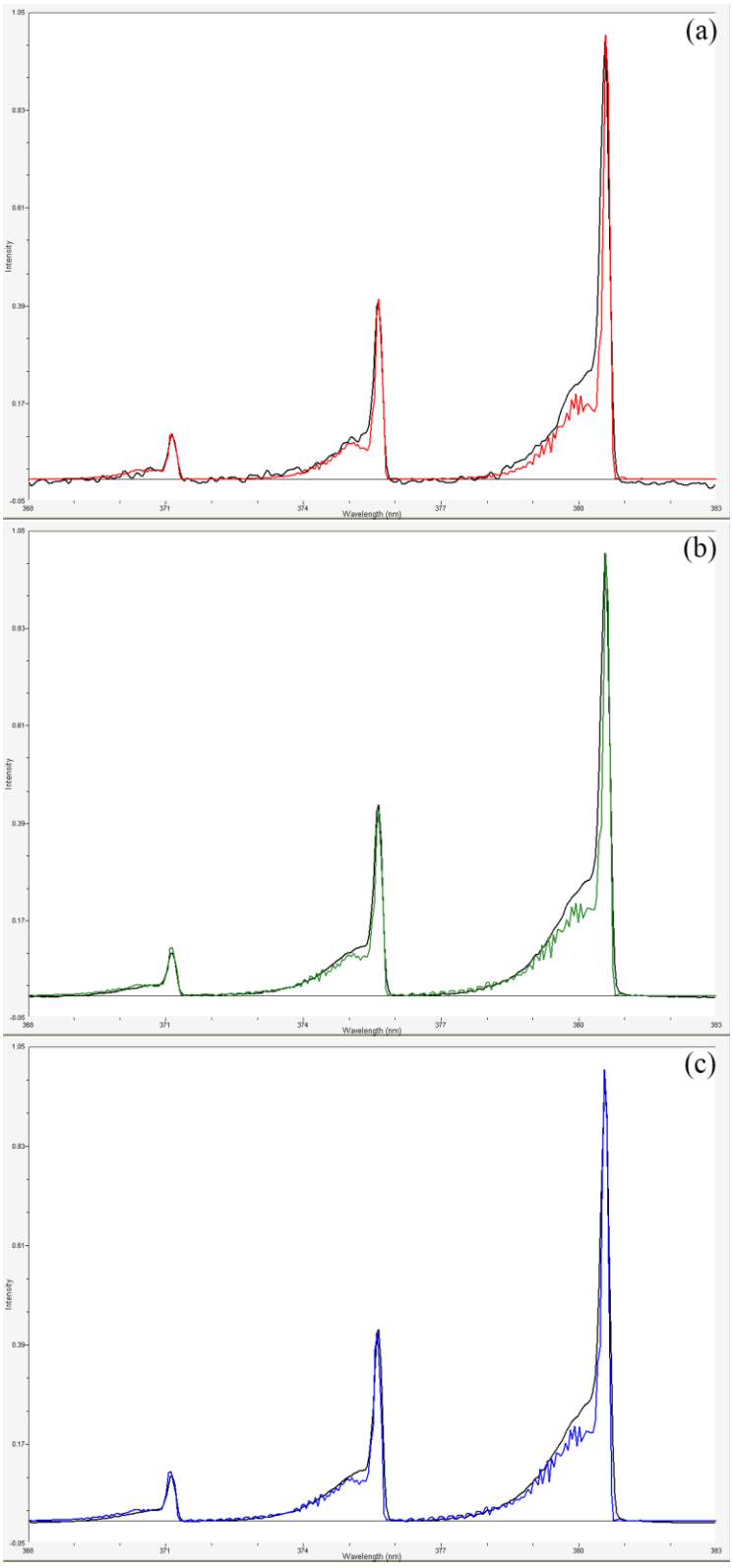

Fig. A.8 Rotational and vibrational temperature fits for OES data produced by (a) 30 kV, (b) 50 kV and (c) 70 kV N_2 plasma estimated by simulations in Specair by peak fitting.

Contact angle measurements after 180 days

Table A.1
Contact angle for constant time samples and constant total dose samples after 180 days.

Sample	Au (°)	Ni (°)
30 kV 5 mins	68.1±0.9	57.6±19.5
50 kV 5 mins	97.3±5.9	73.7±3.3
70 kV 5 mins	120.8±7.1	138.2±17.5
30 kV 3.5 mins	68.8±1.1	64.8±4.1
50 kV 2 mins	69.8±4.7	61.4±2.2
70 kV 1.5 mins	92±7.5	65.2±10.5

Film core volumes measured from optical profilometry

Table A.2
Core volumes of films obtained from optical profilometry images taken at 100× magnification for both constant time samples and constant total dose samples.

Sample	Au (μm)	Ni (μm)
30 kV 5 mins	0.28±0.07	0.85±0.13
50 kV 5 mins	3.85±0.39	3.88±0.28
70 kV 5 mins	1.62±0.15	2.70±0.50
30 kV 3.5 mins	0.05±0.04	0.08±0.01
50 kV 2 mins	1.00±0.23	1.12±0.20
70 kV 1.5 mins	1.67±0.23	2.07±0.23

The core volume, V_{vc}, provides an estimate for the equivalent film thickness. Analysis of V_{vc} shows that the constant-time films are thickest at 50 kV. The constant-dose samples show an increasing trend in thickness with voltage. Overall the thickness is higher for all samples that were dosed for a constant time as compared to the constant-dose samples.

Substrate temperatures during plasma treatment

Table A.3
Substrate temperatures measured by infrared thermometer during plasma exposure.

Sample	Temperature (°C)
30 kV 5 mins	67
50 kV 5 mins	75
70 kV 5 mins	110
30 kV 3.5 mins	60
50 kV 2 mins	65
70 kV 1.5 mins	65

References

1 A.P. Grosvenor, M.C. Biesinger, R.St.C. Smart, N.S. McIntrye, Surf. Sci. 600 (2006) 1771.

2 M.C. Biesinger, B.P. Payne, L.W.M. Lau, A.R. Gerson, R.St.C. Smart, Surf. Interface Anal. 41 (2009) 324.